Electronic Supplementary Information for

Mesostructured organosilica with a 9-mesityl-10-methylacridinium bridging unit: photoinduced charge separation in the organosilica framework

Norihiro Mizoshita, Ken-ichi Yamanaka, Toyoshi Shimada,* Takao Tani and Shinji Inagaki*

Contents

1 General Methods

All manipulations in the precursor synthesis were carried out under a nitrogen atmosphere. Nitrogen gas was dried by passage through P_2O_5. NMR spectra were recorded on a Jeol JNM-EX270 spectrometer at 270 MHz for ^{1}H and 67.5 MHz for ^{13}C. Chemical shifts are reported in δ ppm, referenced to an internal tetramethylsilane standard for ^{1}H NMR and chloroform-*d* (δ 77.0) for ^{13}C NMR. Mass spectra were recorded on a Bruker Daltonics Autoflex mass spectrometer with matrix-assisted laser desorption/ionization (MALDI). UV-vis absorption spectra were obtained on a JASCO V-670 spectrometer. Infrared absorption measurements were conducted on a Thermo Nicolet Avatar 360 FT-IR spectrometer using an attenuated total reflection (ATR) attachment. X-ray diffraction (XRD) measurements were performed on a Rigaku RINT-TTR diffractometer with Cu-Kα radiation (50 kV, 300 mA). Nitrogen adsorption−desorption isotherms were measured using a Quantachrome Autosorb-1 sorptometer at −196 °C. Prior to measurements, all samples were outgassed at 100 °C for 2 h. Brunauer−Emmett−Teller (BET) surface areas were calculated from the linear section of the BET plot ($P/P_0 = 0.05-0.2$). Pore volumes were estimated by the *t*-plot method. Pore size distributions were determined using the density functional theory (DFT) method (the DFT kernel used: N_2 at 77K on silica, cylindrical pore, NLDFT equilibrium model). ^{29}Si magic-angle spinning (MAS) and ^{13}C cross-polarization (CP) MAS NMR spectra of the solid samples were recorded on a Bruker Avance 400 spectrometer (at 79.49 MHz for ^{29}Si and 100.62 MHz for ^{13}C) using 7 mm zirconia rotors and a sample spinning frequency of 4 kHz. The chemical shifts for all spectra were referenced to tetramethylsilane at 0 ppm. Scanning electron microscope (SEM) observation was performed on a Hitachi S-5500 machine with an accelerating voltage of 2.0 kV.

Nanosecond transient absorption measurements were performed under argon atmosphere, using the third-harmonic pulse (355 nm, 7 ns fwhm, 1 Hz) of a Nd^{3+}:YAG laser (Continuum, NY-81) for the excitation light source. A 150 W Xe lamp (Hamamatsu Photonics, L2274) was used as the probe light, which was incident on the sample perpendicular for solution or at a 30-degree angle for films to the excitation light path. The output of the monochromator (Ritsu, MC-10N) was monitored using an avalanche photodiode (Hamamatsu Photonics, S5343 for 320–980 nm; G8931-20 for 940–1600 nm). The signal from the detector was recorded on a digital oscilloscope (Tektronix, TDS3032B). The total system was controlled with a personal computer via a GP-IB interface.

2 Synthesis of Precursor 1

Synthesis of *N*-methoxymethyl-2,7-dibromoacridone (3). To a mixture of 2,7-dibromoacridone (11.6 g, 34.4 mmol) and sodium hydride (60% oil dispersion; 3.50 g, 86.1 mmol) was added distilled DMF (320 mL). The mixture was stirred at room temperature for 30 min and then methoxymethyl chloride (8.4 mL, 110 mmol) was added. The reaction mixture was stirred at 0 °C for 2 h, quenched with water (500 mL), filtered, and washed with hexane (100 mL). The residue was dried in vacuo to give **3** (10.5 g, 80% yield): ^{1}H NMR ($CDCl_3$) δ 3.55 (s, 3H), 5.60 (s, 2H), 7.51 (d, *J* = 9.2 Hz, 2H), 7.79 (dd, *J* = 9.2 Hz, 2.7 Hz, 2H), 8.60 (d, *J* = 2.7 Hz, 2H); ^{13}C NMR ($CDCl_3$) δ 55.90, 78.00, 115.92, 117.31, 123.61, 130.11, 137.05, 141.08, 176.03.

Synthesis of 2,7-dibromo-9-mesitylacridine (4). To a solution of **3** (1.51 g, 3.80 mmol) in THF (108 mL) was added slowly 2-mesitylmagnesium bromide in THF (60 mL), derived from 2-bromomesitylene (2.4 ml, 16.0 mmol) and magnesium turning (440 mg, 18.0 mmol, 1.3 eq.), at 0 °C. The mixture was allowed to stir at room temperature for 24 h and then at 50 °C for 12 h, and quenched carefully with 10% HCl aq. (50 mL) and water (50 mL). The reaction mixture was adjusted to pH 9 with saturated aqueous K_2CO_3 and extracted with CH_2Cl_2 three times. The combined organic layer was washed with saturated NaCl aq., dried over $MgSO_4$, and the solvent was evaporated under reduced pressure. The residue was chromatographed on silica gel (CH_2Cl_2) to give **4** (1.62 g, 94 %): ^{1}H NMR ($CDCl_3$) δ 1.71 (s, 6H), 2.47 (s, 3H), 7.11 (s, 2H), 7.63 (d, *J* = 2.2 Hz, 2H), 7.83 (dd, *J* = 9.2 Hz, 2.2 Hz, 2H), 8.13 (d, *J* = 9.2 Hz, 2H); ^{13}C NMR ($CDCl_3$) δ 19.99, 21.23, 121.01, 126.26, 127.64, 128.78, 130.46, 131.74, 134.09, 136.36, 138.61, 145.36, 147.43.

Synthesis of 2,7-bis(triethoxysilyl)-9-mesitylacridine (5). To a mixture of $[Rh(CH_3CN)_2(cod)]BF_4$ (38 mg, 0.10 mmol), tetrabutylammonium iodide (1.22 g, 3.30 mmol), and **4** (752 mg, 1.65 mmol) was added distilled DMF (26 mL) and triethylamine (1.4 ml, 9.90 mmol). The mixture was stirred at room temperature for 30 min, and then triethoxysilane (1.2 ml, 6.60 mmol) was added dropwise at 0 °C and stirring was continued at 80 °C for 2 h. The reaction mixture was then concentrated under vacuum to remove DMF. The resulting mixture was treated with Et_2O to obtain a solution of **5** in Et_2O, which was filtered through a Celite plug, and the filter cake was rinsed with Et_2O. The combined filtrates were concentrated under vacuum and the residue was passed through charcoal to give **5** (940 mg, 98%): ^{1}H NMR ($CDCl_3$) δ 1.16 (t, *J* = 7.0 Hz, 18H), 1.67 (s, 6H), 2.43 (s, 3H), 3.83 (q, 7.0 Hz, 12H), 7.06 (s, 2H), 7.91 (d, *J* = 1.4 Hz, 2H), 8.01 (dd, *J* = 8.9 Hz, 1.4 Hz, 2H), 8.28 (d, *J* = 8.9 Hz, 2H); ^{13}C NMR ($CDCl_3$) δ 18.04, 19.91, 21.13, 58.86, 124,57, 128.35, 128.89, 128.93, 131.28, 134.58, 135.21, 136.25, 138.10, 148.63, 150.13.

Synthesis of *N*-methyl-2,7-bis(triethoxysilyl)-9-mesitylacridinium trifluoromethane sulfonate (1). To a solution of **5** (950 mg, 1.65 mmol) in CH_2Cl_2 (48 mL) was added dropwise methyl trifluoromethane sulfonate (0.28 ml, 2.48 mmol) at 0 °C, and then stirred at room temperature for 1 h, diluted with EtOH (20 mL), stirred for 10 min, and concentrated to give Mes-Acr^{+} precursor **1** quantitatively: ^{1}H NMR ($CDCl_3$) δ 1.17 (t, *J* = 6.8.0 Hz, 18H), 1.71 (s, 6H), 2.48 (s, 3H), 3.84 (q, 6.8

Hz, 12H), 5.08 (s, 3H), 7.15 (s, 2H), 8.16 (d, *J* = 1.4 Hz, 2H), 8.57 (dd, *J* = 9.5 Hz, 1.4 Hz, 2H), 8.75 (d, *J* = 9.5 Hz, 2H); ^{13}C NMR ($CDCl_3$) δ 17.87, 19.86, 21.03, 38.94, 59.09, 118.22, 120.48 (q, $J_{C\text{-}F}$ = 318.6 Hz), 125.09, 128.794, 128.88, 133.38, 135.55, 136.85, 140.32, 142.25, 143.93, 163.43; MS (MALDI) *m*/*z* calcd for $C_{35}H_{50}NO_6Si_2$ (M^+ – OTf): 636.3171, found 636.3170 (100%).

3 Preparation of Organosilica Films

For the preparation of mesostructured and mesoporous organosilicas, an acidic sol solution consisting of **1**/Brij76/EtOH/H_2O/HCl = 1.0/0.74/855/8.7/0.052 (molar ratio) was stirred at room temperature for 24 h. The sol solution was cast onto a quartz or glass substrate and dried at room temperature under reduced pressure. In order to remove the template surfactant Brij76, the cast film was immersed in EtOH at 50 °C for 12 h, and then dried at room temperature. The removal of Brij76 was confirmed by the disappearance of infrared absorption bands at 2850−2960 cm^{-1} corresponding to C−H stretching modes of alkyl chains of Brij76 (Fig. S1).

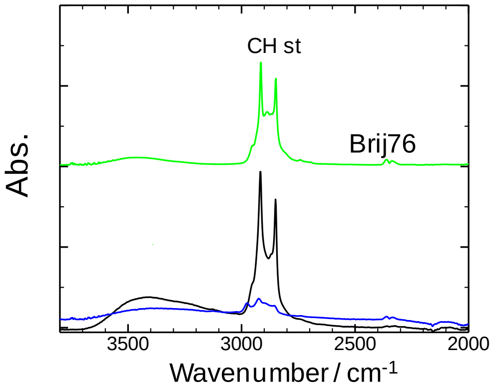

Fig. S1 FT-IR spectra of the mesostructured organosilica films based on **1** before (black) and after removal of Brij76 (blue). The green line shows an FT-IR spectrum of neat Brij76.

A transparent organosilica film of **1** without template surfactant was prepared using a solution consisting of **1**/EtOH/H_2O/HCl = 1.0/2158/28.2/0.25 (molar ratio). The sol solution was stirred at room temperature for 24 h. The solution was cast onto a quartz substrate and dried at 45 °C under reduced pressure.

4 Supplementary Experimental Results

4.1 UV-vis absorption spectra of precursor 1 and sol−gel polycondensed films

UV-vis absorption spectra of **1** (2-propanol solution), a transparent sol−gel polycondensed film, and a mesostructured film were shown in Fig. S2. The spectral shape of the films is close to that of the dilute solution of **1** and those reported in the literature.[1] For the mesostructured film, the baseline is largely shifted upward due to the haze of the film.

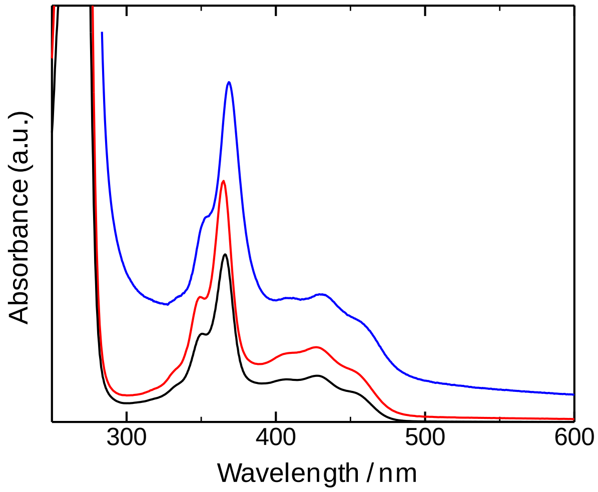

Fig. S2 UV-vis spectra of a 2-propanol solution of **1** (black), a non-structured sol−gel polycondensed film (red) and a mesostructured film (blue).

4.2 Transient absorption spectra of a haze-free non-structured Mes-Acr$^+$–silica film

Fig. S3 shows transient absorption spectra of a transparent Mes-Acr$^+$–silica hybrid film without a surfactant. Irradiation of the film by laser excitation (355 nm, 7 ns pulse) resulted in transient absorption bands at 370 nm and 420–550 nm in microsecond time scale. The spectroscopic behavior is similar to that of the mesostructured film shown in Fig. 2. In this case, the half-life period of the Acr$^\bullet$ species calculated using the absorbance decay at 370 nm is 3.7 μs. These results support that the formation of Acr$^\bullet$ in microsecond time scale originates from the framework composition with a high density of the Mes-Acr$^+$ units.

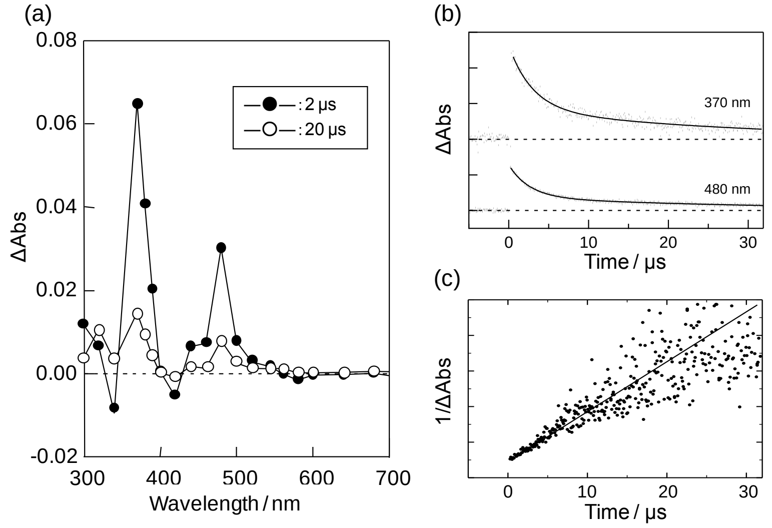

Fig. S3 (a) Transient absorption spectra of the non-structured organosilica film prepared from **1** after laser excitation at 355 nm. (b) Absorbance time profiles at 370 and 480 nm. (c) Time profile of the reciprocal of the absorbance decay at 370 nm.

4.3 Mes-Acr$^+$−silica-catalyzed photooxidation

We preliminarily performed photooxidation reactions of two substrates, benzyl alcohol (BnOH)[2] and triphenylphosphine (TPP),[3] in the presence of the Mes-Acr$^+$−silica hybrid. The Mes-Acr$^+$−silica hybrid after the extraction of Brij76 was ground and thoroughly washed with dichloromethane before the photocatalysis test. The reaction conditions were summarized in Table S1. As for runs A and C, the Mes-Acr$^+$−silica hybrid solid was dispersed in dichloromethane solutions of BnOH and TPP. The reaction mixtures under O_2 bubbling were exposed to visible light (300 W xenon lamp MAX-301 (Asahi Spectra Co., Ltd.), >385 nm) for 12 h. After the Mes-Acr$^+$−silica powders were filtered off, the solvents were evaporated and the residues were analyzed by ^{1}H NMR spectroscopy in $CDCl_3$. As reference samples, only O_2 bubbling was performed for the solutions of the substrates (runs B and D).

Table S1. Preliminary oxidation reaction catalyzed by Mes-Acr$^+$-silica hybrids

run	Reaction conditions
A	BnOH (100 mg)/Mes-Acr$^+$-silica (5 mg)/CH_2Cl_2 (3 mL), O_2 bubbling, light irradiation, 12 h
B	BnOH (100 mg)/CH_2Cl_2 (3 mL), O_2 bubbling, 12 h
C	TPP (100 mg)/Mes-Acr$^+$-silica (5 mg)/CH_2Cl_2 (3 mL), O_2 bubbling, light irradiation, 12 h
D	TPP (100 mg)/CH_2Cl_2 (3 mL), O_2 bubbling, 12 h

Photooxidized products, benzaldehyde and triphenylphosphine oxide, were yielded in the reaction mixtures as seen in the ^{1}H NMR spectra of runs A and C (Fig. S4). For runs B and D, no oxidized products were detected. Although the reaction efficiency of runs A and C was low (conversions of the substrates: 2.9% for BnOH and 7.1% for TPP) in the present stage due to no optimization of the reaction conditions including particle size of the organosilica solid and light irradiation methods, the photocatalytic activity of the Mes-Acr$^+$ bridging group was confirmed to work in the solid silica matrices. The NMR spectra of runs A and C also show no leaching of Mes-Acr$^+$ units from silica matrices into solutions during the reactions.

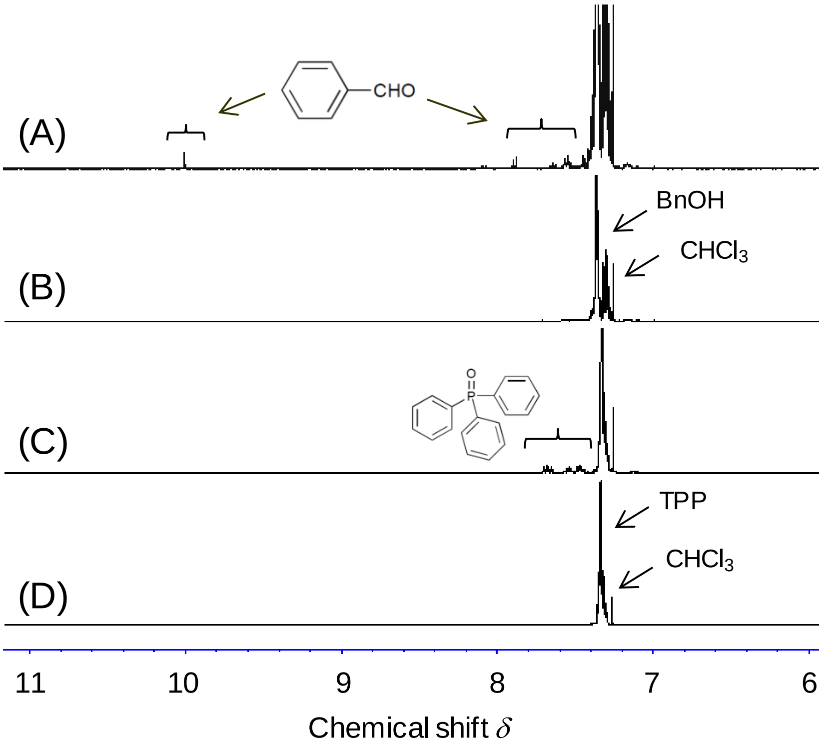

Fig. S4 ^{1}H NMR spectra of residual compounds obtained from runs A−D.

4.4 Solid-state NMR measurements of Mes-Acr$^+$–silica hybrid

Fig. S5 show ^{13}C CP MAS and ^{29}Si MAS NMR spectra of the Mes-Acr$^+$–silica hybrid after the extraction of the template surfactant. For the ^{13}C CP MAS NMR spectrum, the peaks from 119.2 to 143.3 ppm correspond to aromatic carbons of the Mes-Acr$^+$ moiety and the chemical shifts are in agreement with those of the precursor compound **1**. Two intense peaks at 19.8 and 38.9 ppm are characteristic of methyl substituents of Mes and Acr$^+$ moieties, respectively, which confirms that the Mes-Acr$^+$ groups are intact in the film. ^{29}Si MAS NMR spectrum indicates that the framework is rich in T^2 species (R-*Si*(OSi)$_2$(OH)). This is reasonable because the polycondensation of the precursor proceeded in a weak acidic condition. On the other hand, a small amount of Q species generated by

Si–C bond cleavage is observed at –90 to –112 ppm. Although the Q species slightly yielded in the polycondensation process, further Si–C bond cleavage did not occur during post-treatments and no leaching was observed in catalytic reaction test. These results suggest that the Mes-Acr$^+$ units are properly fixed on the silica framework.

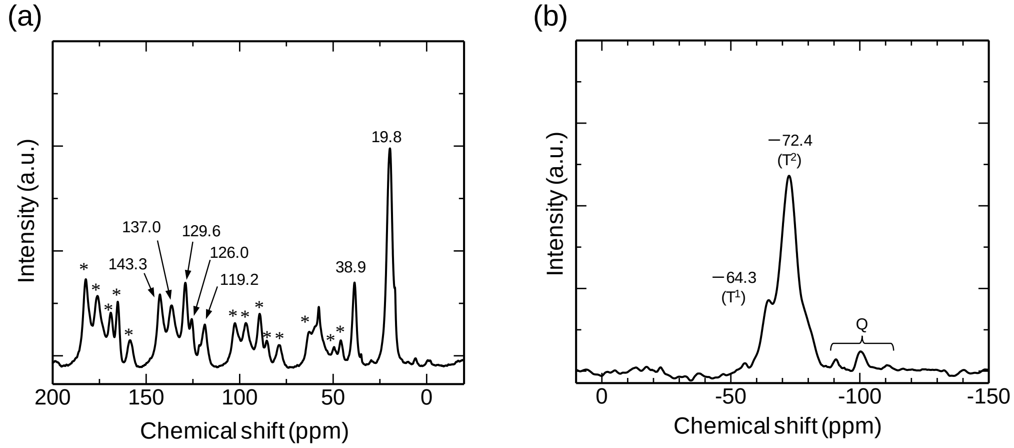

Fig. S5 (a) ^{13}C CP MAS and (b) ^{29}Si MAS NMR spectra of the Mes-Acr$^+$–silica hybrid film after the extraction of the template surfactant. Asterisk (*) indicates spinning sidebands.

4.5 SEM observation of the mesostructured Mes-Acr$^+$–silica hybrid

Fig. S6 shows SEM images of the mesostructured Mes-Acr$^+$–silica hybrid film prepared on silicon wafers. Fig. S6a indicates the formation of submicrometer-scale grains in the film, which may cause the haze of the thick film. On the surface of the grains, porous structures with 4–10 nm in diameters are observed as shown in Fig. S6b. However, we failed to obtain clearer images due to the damage of the films. During electron beam irradiation, moving and deformation of the organosilica samples occurred, which made it difficult to perform electron microscope observation, in particular, at high magnification.

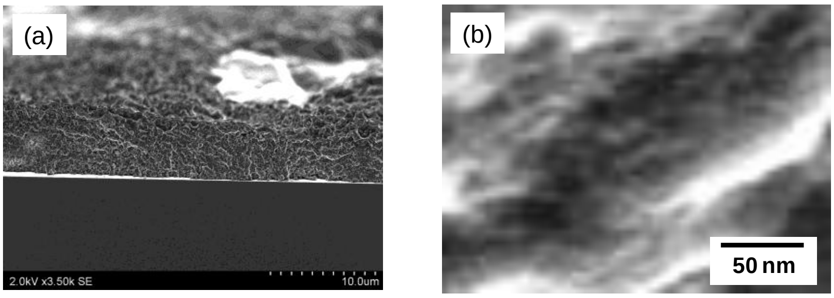

Fig. S6 SEM images of a cross section of a thick Mes-Acr$^+$–silica hybrid film ((b) is digitally zoomed from an image obtained at low magnification).

4.6 Nitrogen adsorption–desorption isotherm of mesoporous Mes-Acr$^+$–silica hybrid

For the sample preparation, the as-synthesized Mes-Acr$^+$–silica hybrid film formed on a glass substrate was exposed to vapor of 28% NH_3 aqueous solution at 60 °C for 2 h to reinforce the organosilica framework. After the extraction of the template surfactant, the film was peeled off from the substrates and ground. Fig. S7 shows a nitrogen adsorption–desorption isotherm of the Mes-Acr$^+$–silica hybrid. The isotherm is classified as type-IV typical of mesoporous materials. The BET surface area, pore volume and pore diameter are 910 m^2 g^{-1}, 0.55 cm^3 g^{-1} and ca. 3.7 nm, respectively. The broad pore size distribution (Fig. S7, inset) is probably due to partial collapse of the mesostructure by extracting the template surfactant and peeling off from the substrate.

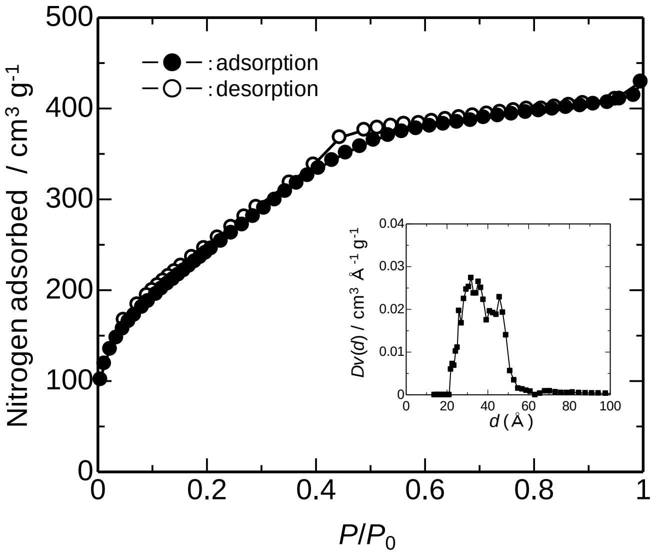

Fig. S7 Nitrogen adsorption–desorption isotherm of the mesoporous Mes-Acr$^+$–silica hybrid. Inset shows the pore size distribution.

References

1. K. Ohkubo, H. Kotani and S. Fukuzumi, *Chem. Commun.*, 2005, 4520−4522.
2. K. Ohkubo, K. Suga and S. Fukuzumi, *Chem. Commun.*, 2006, 2018−2020.
3. K. Ohkubo, T. Nanjo and S. Fukuzumi, *Bull. Chem. Soc. Jpn.*, 2006, **79**, 1489−1500.